Check for updates

Ultrasensitive determination of ascorbic acid by using cobalt oxyhydroxide nanosheets to enhance the chemiluminescence of the luminol–H₂O₂ system†

Huihui Xu,[a] Qiyong Cai,[a] Qiuyu Nie,[a] Zhun Qiao,[a] Song Liu [ID] *[a] and Zhaohui Li [ID] *[b]

Ascorbic acid (AA) as an essential vitamin in the human body participates in various physiological reactions and plays a key role in many biochemical processes. Therefore, it is of vital importance to monitor and quantify AA in commercial tablets, beverages and food. In this work, a rapid and ultrasensitive chemiluminescence (CL) system for the detection of AA was developed, in which ultrathin cobalt oxyhydroxide (CoOOH) nanosheets were applied in the conventional luminol–H₂O₂ CL system. The results showed that ultrathin CoOOH nanosheets as a catalyzer remarkably improved the CL intensity of the CoOOH–luminol–H₂O₂ system, up to about 1400-fold. Under the optimized conditions, the CL inhibition efficiencies increase linearly with the concentrations of AA in the range of 1–500 pmol L⁻¹, and the limit of detection was 39 fmol L⁻¹. Moreover, the proposed CL system was successfully applied in the determination of AA in medicinal tablets with satisfactory results.

Introduction

Ascorbic acid (AA), also called vitamin C or ascorbate, is a common water soluble organic compound involved in many biological processes and metabolisms.[1] As an essential micronutrient, AA plays an essential role in human and animal metabolic process,[2,3] and it is often used as an antioxidant added to food, beverages and medicinal preparations.[4] The shortage of AA results in scurvy, and the excessive intake of AA can lead to stomach convulsions, urinary stones and diarrhea. Therefore, the rapid, sensitive, and selective detection of AA levels is of significance in the cases of medical assays and diagnosis.

Up to now, a wide variety of analytical techniques have been developed to detect and quantify ascorbic acid, such as fluorimetry,[4–6] chromatography,[7,8] spectrometry,[9] colorimetry,[10,11] and electrochemistry.[12,13] Yan's group developed a CdTe QD fluorescent probe for the selective detection of AA after quenching by a certain amount of KMnO₄ with the limit of detection of 74 nmol L⁻¹.[14] Zhang *et al.* have constructed a highly sensitive, selective electrochemical sensor for the

determination of AA *via* the combination of a functionalized multi-walled carbon nanotube layer with a thin molecularly imprinted polymer (MIP) film. The integration of MIT in organic electrochemical transistor sensors (OECTs) is a reasonably effective route to improve the selectivity and applicability of OECTs in biosensors.[15] Although these methods are highly sensitive, most of them suffer disadvantages such as expensive cost, time-consuming, a complicated pretreatment process and the operation of sophisticated instruments, which limit their wide applications. Compared with other methods, chemiluminescence (CL) sensors do not need an excitation source and the corresponding spectrometric systems. Many drawbacks of fluorescence sensors will be avoided including photobleaching and autofluorescence. These advantages of CL sensors greatly improve the sensitivity. Conventional and primary CL systems including luminol, acridinium ester, AMPPT, potassium permanganate and Ce(iv) have got extensive development and applications. All these methods have been used for detecting AA such as luminol–K₃Fe(CN)₆–GNPs,[16] cerium(iv)–rhodamine B CL system,[17] luminol–H₂O₂–gold colloids system,[18] and Mg–Al–CO₃ LDHs-catalyzed ONOOH system.[19] The luminol–H₂O₂ system, as a popular and classic CL reaction, has been extensively investigated. It can be catalyzed by metal ions, nanoparticles, graphene oxide and peroxidases. However, there are still some shortcomings of these catalysts, such as high toxicity and cost for metal ions and metal nanoparticles, complicated synthetic steps for graphene oxide, and low stability for peroxidases.

[a]Institute of Chemical Biology and Nanomedicine (ICBN), State Key Laboratory of Chemo/Biosensing and Chemometrics, College of Chemistry and Chemical Engineering, Hunan University, Changsha, 410082, P. R. China. E-mail: liusong@ hnu.edu.cn

[b]College of Chemistry and Molecular Engineering, Zhengzhou University, Zhengzhou 450001, P. R. China. E-mail: zhaohui.li@zzu.edu.cn

† Electronic supplementary information (ESI) available: Additional figures. See DOI: 10.1039/c8ra03528h

In recent years, cobalt oxyhydroxide (CoOOH) nanosheets are known by its rich electrical and catalytic properties,[20] which were explored in sensing of AA. For example, Li *et al.* developed a novel strategy on the basis of the specific reaction of CoOOH and AA for detection and imaging of AA in living cells and *in vivo*.[21] CoOOH nanoflakes can quench the luminescence of persistent luminescence nanoparticles (PLNPs), the presence of AA can reduce CoOOH into Co^{2+} and the luminescence was recovered. Recently, Cui *et al.* reported that under the weak acidic condition and in the absence of hydrogen peroxide, CoOOH nanosheets can catalyze the 3,3′,5,5′-tetramethylbenzidine (TMB) to produce blue solution which could reduce the fluorescence intensity of albumin-stabilized gold nanoclusters (BSA-AuNCs). The addition of ascorbic acid destroyed some of the CoOOH nanosheets and retarded the catalytic oxidation, in hence, less fluorescence was reduced.[22] Yao's group proposed a novel label-free fluorescent sensing system to detect alkaline phosphatase (ALP) which can catalyze L-ascorbic acid-2-phosphate into AA based on chemical redox strategy to modulate the fluorescence of nitrogen-doped graphene quantum dots (NGQDs).[23] It is worthy to note that all these are turn-on fluorescence probes.[24] However, the limited quenching capability of CoOOH nanosheets and the deficiency in fluorescence resonance energy transfer between CoOOH nanosheets and fluorescent materials led to the low sensitivity of these methods. In addition, in fluorescence detection an external light source is required.

In this work, the enhancing CL of luminol–H_2O_2 system was built for AA detection in the presence of CoOOH nanosheets. To the best of our knowledge, it is the first time that CoOOH nanosheets were applied in CL system. The prepared ultrasensitive CoOOH nanosheets exhibited excellent catalytic property on CL system. On the basis of the mechanism demonstrated in Scheme 1 the enhancing CL method for AA detection was developed. The results showed that CoOOH nanosheets have a remarkably enhancing effect on the CL of luminol–H_2O_2 system when its concentration is low. AA can reduce the CoOOH nanosheets to Co^{2+} and inhibit the CL of luminol–H_2O_2 enabling the ultrasensitive detection of AA with the limit of detection as 39 fmol L^{-1}. This work provides an ultrasensitive, simple and rapid route to construct CoOOH–luminol–H_2O_2 CL sensor, which has been successfully applied to the detection of AA in medicinal tablets with satisfactory results. Due to the fascinating properties of the modified CL system including ultrasensitive, simple, low consumption and easy to operate, it was anticipated that in the near future the method would has promising applications in sensitive detection of target analytes.

Experimental procedures

Reagents and materials

Ascorbic acid (reduced form), luminol, hydrogen peroxide (H_2O_2), cobalt chloride ($CoCl_2$), sodium hypochlorite (NaClO), amino acids, and Tris (hydroxymethyl) aminomethane (Tris–HCl) were obtained from Sigma-Aldrich (St. Louis, MO, USA). Vitamin C tablets were purchased from BY-HEALTH Co., Ltd. (Zhuhai, China). A 10^{-2} mol L^{-1} luminol solution was prepared
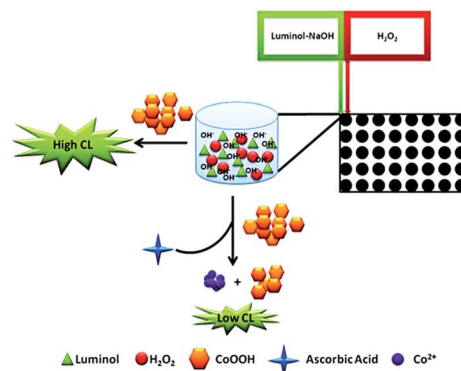
Scheme 1 Schematic illustration for AA detection by using CoOOH enhanced luminol–H_2O_2 CL system.

by dissolving 177.1 mg of luminol in 100 mL of 0.1 mol L^{-1} NaOH solution and stocked at 4 °C. A stock solution of 5×10^{-2} mol L^{-1} H_2O_2 was prepared by diluting 1.5 mL of 30% (v/v) H_2O_2 to 13.5 mL with ultrapure water. Standard solutions of ascorbic acid were prepared daily in ultrapure water. All other reagents were analytical grade without further treatment and purchased from Aladdin reagent Co., Ltd. (Shanghai, China). All solutions were prepared using ultrapure water generated from an ELGA Labwater system (US) with an electrical resistance ≥ 18.2 MΩ. Morphology images of CoOOH nanosheets were photographed by transmission electron microscope (JEOL 2100 plus, Japan) at an accelerating voltage of 200 kV. A drop of sample solution was placed on a copper grid that was let to dry before being transferred into the TEM sample chamber. Fourier Transform Infrared Spectrometer (FTIR) results were tested on the IRAffinity-1 (SHIMADZU, Japan). Chemiluminescence was measured on the Spark 10M Microplate Reader (Bio-Tek, Winooski, VT). The UV-vis absorption spectra were collected on a Cary 60 UV-vis spectrometer (Agilent Technologies, USA). The crystal structure was identified by XRD-6100 (SHIMADZU, Japan). Zeta-sizer Nano (Malvern) was used to measure hydrodynamic size and zeta potential CoOOH-nanosheets. All the pH was performed with a Leici PHS-3C meter (Leici, Shanghai, China).

Preparation of CoOOH nanosheets

CoOOH nanosheets were synthesized by following the previous articles with slight modifications.[23] In brief, 3 mL of NaOH (1 mol L^{-1}) was added to 20 mL of $CoCl_2$ (5 mmol L^{-1}) solution, subsequently, sonicated for 1 min. Then, 500 μL of NaClO (0.9 mol L^{-1}) was added to the mixture and sonicated for 10 min. After that the product was collected by centrifugation at 10 619 × *g* for 15 min, washed with ultrapure water for three times and freeze drying for 12 h. Finally, the power of CoOOH nanosheets was redispersed in ultrapure water with the aid of ultrasonic.

CL measurements of AA

The chemiluminescence sensing of AA were all performed in Tris–HCl buffer (10 mmol L^{-1}, pH 9.5). Typically, 250 ng mL^{-1}

CoOOH nanosheets solution and ascorbic acid solutions (0–10 nmol L^{-1}) were added into 130 μL of 10 mmol L^{-1} Tris–HCl buffer (pH 9.5) in each well of the microtiter plate. Then the pumps were washed for three times with 10^{-4} mol L^{-1} luminol and 0.1 mol L^{-1} H$_2$O$_2$. Afterwards, luminol solution and H$_2$O$_2$ solution with the flow injection rates of 200 μL s^{-1} were injected into the target microtiter plate well. The specific schematic diagram of flow injection was illustrated in Scheme 1. The CL signals were monitored by PMT adjacent to the CL flow-through column. The signals were imported to the computer for data acquisition. The relative CL intensity {(CL$_0$ − CL)/CL$_0$} was used for calibration and quantification of AA, where CL$_0$ and CL represented the CL intensities with and without adding AA, respectively.

Selectivity

To investigate the selectivity of the proposed method, the response of the system to 10 pmol L^{-1} AA and 100 pmol L^{-1} potential interferences which were prepared in ultrawater were tested. The interferences we tested are including twelve different kinds of amino acids (Trp, Gly, Phe, Ile, Val, Asp, Arg, Tyr, Cys, His, Leu, Lys), seven kinds of electrolytes (ZnSO$_4$, MgSO$_4$, CaCl$_2$, KCl, NaCl, AlCl$_3$, CoCl$_2$), glucose, sucrose and dopamine (DA). Subsequently, the CL intensity of the interfering species was recorded by utilizing Spark 10M Reader.

Detection of AA in commercial tablets samples

In order to study the detection performance of the method in practical applications, commercial vitamin C tablets were investigated. The vitamin C tablet was crushed in a pestle and mortar. The crushed powder (1.0 g) was weighed accurately and dissolved in 50 mL ultrapure water with ultrasonication. Then the solution was centrifuged at 10 619 × g for 15 min to remove the insoluble impurities. Afterwards, the resulting solution was diluted 10^7 fold with ultrapure water to make sure the AA concentration fall into the detection range. Then 20 μL AA (200 pmol L^{-1}, 1 nmol L^{-1}, and 2 nmol L^{-1}) was mixed with 130 μL diluted tablet solutions in the appointed well of the microtiter plate, and 10 μL CoOOH nanosheets (2.5 μg mL^{-1}) were added. The assay conditions used were the same as mentioned above for detecting AA in vitamin tablets.

Results and discussion

Preparation and characterization of CoOOH nanosheets

Under the alkaline condition, CoCl$_2$ can react with NaClO to form ultrathin CoOOH nanosheets. To investigate the morphology of the CoOOH nanosheets, the TEM assay was performed. As shown in Fig. 1A, the CoOOH nanosheets had the typical hexagon morphology with the particles size around 80 to 100 nm. Simultaneously, the DLS investigated the size of the CoOOH nanosheets and indicated that the particle size of the prepared CoOOH nanosheets is uniform (Fig. 1B). The zeta potential of the CoOOH nanosheets was 15.02 mV, showing the positive charge of the nanosheets (Fig. S1†), which was attributed to its innovative properties of high conductivity,
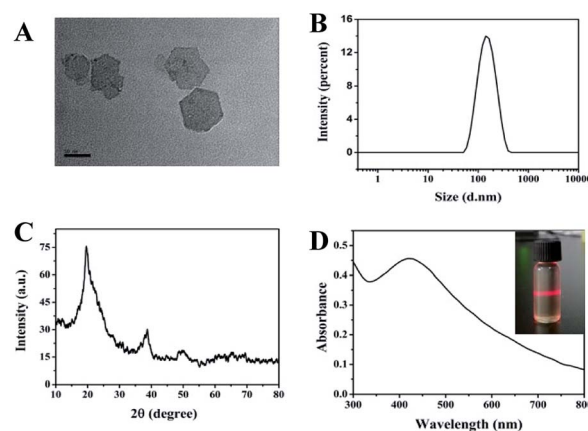

Fig. 1 (A) TEM image of CoOOH. (B) DLS measurements of CoOOH nanosheets. (C) XRD pattern of the CoOOH nanosheets. (D) UV-vis absorption spectra of CoOOH nanosheets (inset: the Tyndall effect of the CoOOH nanosheets solution).
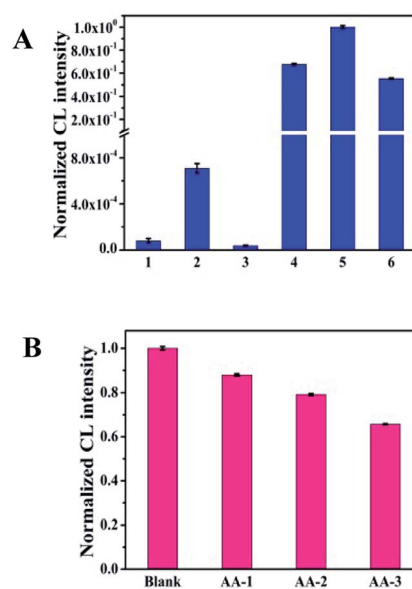

Fig. 2 (A) Effect of CoOOH on the CL intensity: luminol system; luminol–H$_2$O$_2$ system; luminol–CoOOH system; luminol–H$_2$O$_2$–Co^{2+} (the concentration of Co^{2+} is 2.5 × 10^{-7} g mL^{-1}); luminol–H$_2$O$_2$–CoOOH system; luminol–H$_2$O$_2$–CoOOH–AA system (the concentration of AA is 100 nmol L^{-1}). (B) The CoOOH enhanced luminol–H$_2$O$_2$ CL system responsed to different concentrations of AA: the concentration of AA is 0, 10^{-12}, 10^{-11}, 10^{-10} mol L^{-1}, respectively. Conditions: luminol: 10^{-4} mol L^{-1}; H$_2$O$_2$: 10^{-2} mol L^{-1}; NaOH: 0.01 mol L^{-1}; CoOOH: 2.5 × 10^{-7} g mL^{-1}; pH 9.5; Tris–HCl, 10 mmol L^{-1}; flow velocity, pump A: 200 μL s^{-1}; pump B: 200 μL s^{-1}. The error bar represents standard deviation of three replicate measurements.

morphology control nature of micrometer/nanometer scale. The power XRD patterns (Fig. 1C) reveal that the crystalline nature of the prepared CoOOH nanosheets is hexagonal system and highly crystalline in nature without any impurities. The characteristic peaks corresponding to the rhombohedral heterogenite structure which in agreement with the standard JCPDS 07-0169.[25] The UV-vis absorption spectra result of
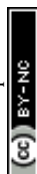
CoOOH nanosheets is showed in Fig. 1D, which has an absorption around 420 nm.[22] The inserted image indicated that the CoOOH nanosheets solution has a good dispersibility and possess the Tyndall effect of the colloidal solution. The FTIR spectrum of CoOOH nanosheets (Fig. S2†) has three characteristic peaks at 3472, 1622, and 615 in the range of 4000–500 cm^{-1}, corresponding to the bond stretching of the hydrogen–bonded hydroxyl group (–OH), the characteristic of the Co–O double bond, and the Co–O^{2-} complex in the oxide.[26] The AFM image shows that the particle size of CoOOH nanosheets is around 100 nm (Fig. S3†), which is confirms the result of Fig. 1B. Therefore, all of these results suggest that our CoOOH nanosheets were successful prepared.

The feasibility and mechanism of CoOOH nanosheets enhanced luminol–H_2O_2 CL system to detect AA

In order to research the feasibility of the CoOOH enhanced luminol–H_2O_2 CL system, we recorded the CL intensity of the individual luminol solution, luminol–H_2O_2 system, luminol–CoOOH system, luminol–H_2O_2–Co^{2+} system, luminol–H_2O_2–CoOOH, luminol–H_2O_2–CoOOH–AA system respectively (Fig. 2A). The results clarified that the ultrathin CoOOH nanosheets can significantly enhance the luminescence intensity of the classic luminol–H_2O_2 system, up to about 1400-fold. At the same time, compared to CoOOH, Co^{2+} has a relative low enhancement effect on the luminol–H_2O_2 system. From Fig. 2B we can observe that the CL intensity decreased with the increase of the concentration of AA, which can be reckoned as the luminol–H_2O_2–CoOOH system can detect AA successfully. The mechanism of luminol–H_2O_2 system has been widely explored, it is generally believed that luminol loses a H^+ ion in alkaline solution and becomes a negatively charged group i.e. 3-aminophthalic acid ion with the oxidation of H_2O_2. The chemical energy generated in the oxidation process and was absorbed by 3-aminophthalic acid ions in an excited state. Then the valence electrons of the oxidation state are changed from the lowest vibrational level of the first electron excited state of the single line to each of the different vibrational levels of the ground state, it will produce the maximum wavelength of 425 nm. In order to explore the possible mechanism of the CL system, we measured the luminescence spectra of luminol–H_2O_2 and luminol–H_2O_2–CoOOH CL system by fluorescence spectrometer. As shown in Fig. S4,† after addition of CoOOH, the maximum wavelength of emission was still 425 nm, indicating that the luminophore of this system is still excited 3-aminophthalate ion. Therefore, the addition of CoOOH nanosheets did not lead to the generation of a new luminophor for the CL system. Thus, the enhanced CL signals may due to the possible peroxidise-like activity of CoOOH nanosheets. In Scheme 2 we proposed the possible mechanism of the luminol–H_2O_2–CoOOH CL system. Under alkaline condition, luminol can be transformed into luminol radial. It is possible that CoOOH nanosheets possess peroxidise-like activity could catalyze H_2O_2 to generate active intermediates such as $OH^{\cdot}$ and $O_2^{\cdot-}$. Luminol radical reacts with active intermediates yield 3-aminophthalate anion and produce the maximum wavelength of 425 nm. The
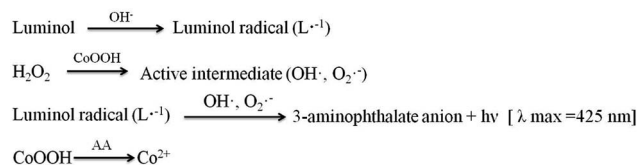
Scheme 2 Possible mechanism of luminol–H_2O_2–CoOOH CL system.
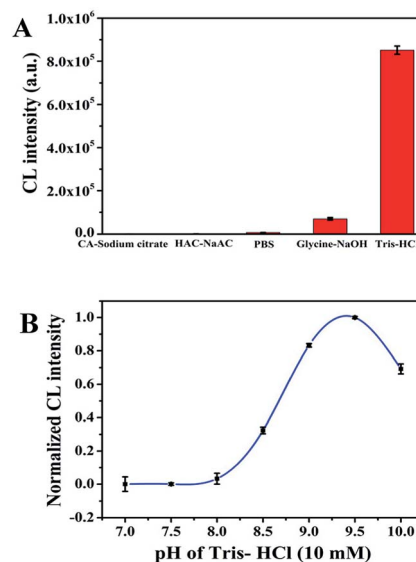
Fig. 3 The influence of reaction conditions on the CL intensity of the CoOOH enhanced luminol–H_2O_2 CL system. (A) Effect of buffer solution (the concentrations of all the buffer solution are 10 mmol L^{-1}): luminol, 10^{-4} mol L^{-1}; H_2O_2, 0.01 mol L^{-1}; pH 10; CoOOH, 2.5 × 10^{-7} g mL^{-1}; flow velocity, pump A: 200 μL s^{-1}; pump B: 200 μL s^{-1}. (B) Effect of buffer pH: luminol, 10^{-4} mol L^{-1}; H_2O_2, 0.01 mol L^{-1}; Tris–HCl, 10 mM; CoOOH, 2.5 × 10^{-7} g mL^{-1}; flow velocity, pump A: 200 μL s^{-1}; pump B: 200 μL s^{-1}. The error bar represents standard deviation of three replicate measurements.

addition of AA can reduce CoOOH into Co^{2+}, which inhibit the catalyze effect of transform H_2O_2 into active intermediates. The results showed in Fig. 2 demonstrated that the conventional luminol–H_2O_2 CL system based on CoOOH nanosheets can be successfully used to detect the concentration of AA.

Optimization of experimental conditions

To acquire credible and reliable results, we optimized different kinds of experimental conditions including the concentration of H_2O_2, the concentration of CoOOH, the optimum buffer, the buffer pH and the optimal flow velocity. The experimental result showed in Fig. S5† indicates that when the concentration of H_2O_2 was in the range of 0.00 to 0.1 mol L^{-1}, the CL signal increased and reaches the maximum value while the concentration is 0.01 mol L^{-1}, after that the CL signal starts to decrease. Therefore, 0.01 mol L^{-1} was chose as the best concentration of H_2O_2. Fig. S6† showed that the CL intensity is the largest when the concentration of CoOOH is 250 ng mL^{-1}, so we chose 250 ng mL^{-1} as the optimal concentration of
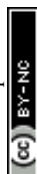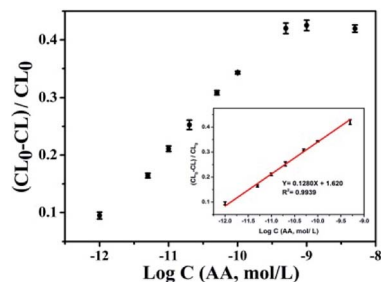
Fig. 4 Plot of relative CL intensity against AA concentration (inset: linear relationship between $(CL_0 - CL)/CL_0$ and log concentration of AA). Conditions: luminol, 1×10^{-4} mol L^{-1}; H$_2$O$_2$, 0.01 mol L^{-1}; Tris–HCl 10 mmol L^{-1}; pH 9.5; CoOOH, 2.5×10^{-7} g mL^{-1}; flow velocity, pump A: 200 μL s^{-1}; pump B: 200 μL s^{-1}. CL_0 represents the CL intensity without AA, and CL represents the CL intensity with different concentrations of AA. The error bar represents standard deviation of three replicate measurements.
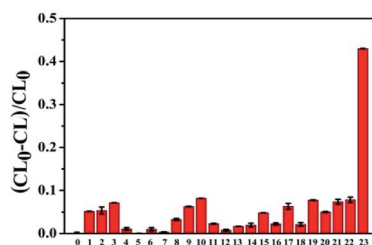

Fig. 5 Relative CL intensity of CoOOH enhanced luminol–H$_2$O$_2$ CL system in the presence of 100 pmol L^{-1} potential interferents and 10 pmol L^{-1} AA. From left to right: blank, tryptophan, glycine, phenylalanine, isoleucine, valine, aspartic acid, arginine, tyrosine, tyrosine, histidine, leucine, lysine, glucose, sucrose, dopamine, ZnSO$_4$, MgSO$_4$, CaCl$_2$, KCl, NaCl, AlCl$_3$, CoCl$_2$, AA. Conditions: luminol, 1×10^{-4} mol L^{-1}; H$_2$O$_2$, 0.01 mol L^{-1}; Tris–HCl 10 mmol L^{-1}; pH 9.5; CoOOH, 2.5×10^{-7} g mL^{-1}; flow velocity, pump A: 200 μL s^{-1}; pump B: 200 μL s^{-1}. The error bar represents standard deviation of three replicate measurements.

CoOOH. In order to investigate the effect of buffer on the system CL intensity we chose five different kinds of buffer solutions, we can observed from Fig. 3A that while the buffer is Tris–HCl the CL signal is the highest, so we chose Tris–HCl as the appropriate buffer for the CL system. We also investigated the pH of buffer, Fig. 3B illustrated that when the Tris–HCl buffer is 9.5 the CL intensity is the highest. Thus, 9.5 was chosen as the optimal pH in the following experiments. As for the flow velocity, we can observe from Fig. S7† that there is no significant variation of CL intensity between different flow rates. As a result, we finally chose the default value (pump A: 200 μL s^{-1};

pump B: 200 μL s^{-1}) as the optimal flow velocity for the follow-up experiments.

Detection of ascorbic acid based on CoOOH nanosheets enhanced luminol–H$_2$O$_2$ CL system

In order to ascertain the application of the CL system to quantify ascorbic acid, under the optimal experimental conditions we measured the CL response of CoOOH enhanced luminol–H$_2$O$_2$ system after reaction with ascorbic acid. Fig. 4 shows the relative CL intensity against AA concentration, we observed that when the concentration of AA attains to 500 pmol L^{-1} the CL intensity intended to be steady, which means the sensing recovery reached the maximum. Moreover, a good linear relationship between $(CL_0 - CL)/CL_0$ and AA concentration which ranging from 1 pmol L^{-1} to 500 pmol L^{-1} with a correlation coefficient square of 0.9939 was obtained (inset in Fig. 4), where CL_0 and CL represented the absence and presence of AA, respectively. In addition, we also describe a comparison about the performance of this approach with previously recommended methods for AA determination in ESI Table S1.† The result indicates that the sensitivity is higher than many previous methods. Furthermore, the CoOOH nanosheets enhanced luminol–H$_2$O$_2$ CL system can be applied to the determination of AA in various real samples.

Selectivity of CoOOH nanosheets enhanced luminol–H$_2$O$_2$ CL system for AA detection

Selectivity is an important factor to evaluate the CL system for detecting AA, because of the complexity of the tested environment, multitudinous coexistent such as common amino acids, electrolytes and other biological molecules would have a negative effect on the AA detection. Several interfering substances including amino acids (Trp, Gly, Phe, Ile, Val, Asp, Arg, Tyr, Cys, His, Leu, Lys), electrolytes (ZnSO$_4$, MgSO$_4$, CaCl$_2$, KCl, NaCl, AlCl$_3$, CoCl$_2$) and some small biomolecules (glucose, sucrose and dopamine) were assessed under the optimal experimental conditions. As shown in Fig. 5, whether amino acids, electrolytes or small biological molecules do not generate an obvious and apparent interference on the proposed luminescence system even though the concentration of these interferents is 10 fold higher than that of AA. Therefore, this CL system based on CoOOH nanosheets could be applied for detecting AA in medicinal tablets or food samples directly.

Detection of ascorbic acid in commercial tablets

In order to explore the feasibility of this proposed procedure in complicated real sample environment, the assay was then

Table 1 Analytical results of determination of ascorbic acid in medicinal tablets samples

Sample	Claimed (pmol L^{-1})	Initial amount (pmol L^{-1})	Added amount (pmol L^{-1})	Fund (pmol L^{-1})	Recovery (%)	RSD ($n = 3$, %)
1	241.9	235.7	20	254.7	95.0	1.29
2			100	334.3	98.6	1.56
3			200	428.5	96.4	1.44

applied to detect AA spiked in diluted medical tablets. The tablets were dissolved, diluted and then spiked into three different kinds of concentration of AA. The content of AA in tablets was determined by this proposed method. As shown in Table 1, the recoveries of the spiked amounts of AA in diluted medical tablets solutions were obtained in the range of 95.0–98.6% with relative standard deviations (RSDs) below 1.56% for the real sample. These results proved that this CL sensing system based on CoOOH nanosheets–luminol–H_2O_2 was likely to be capable of real sample analysis.

Conclusions

In this work, the ultrathin CoOOH nanosheets were firstly found which hold the ability of enchancing the chemiluminescence performance of the conventional luminol–H_2O_2 system. The enhanced CL ability was ascribed to the possible peroxidise-like activity of CoOOH nanosheets. Based on this principle, this method shows strong detection ability for AA with ultrasensitivity and good selectivity. Meanwhile, this assay could not only function in aqueous solution for AA detection but also exhibit reliable responses toward AA in real samples. Taking full advantages of CoOOH nanosheets–luminol–H_2O_2 CL system, this assay shows remarkable properties including ultrasensitive, fast, simple, and cost-effective as well as environmental-friendly, which suggest that this strategy has a great potential to be utilized as an efficient tool for determination of AA level in biological environments.

Conflicts of interest

There are no conflicts to declare.

Acknowledgements

References

1 Z. Gazdik, O. Zitka, J. Petrlova, *et al.* Determination of vitamin C (ascorbic acid) using high performance liquid chromatography coupled with electrochemical detection, *Sensors*, 2008, **8**, 7097–7112.

2 Y. Hu, L. Zhang, X. Geng, *et al.* A rapid and sensitive turn-on fluorescent probe for ascorbic acid detection based on carbon dots–MnO_2 nanocomposites, *Anal. Methods*, 2017, **9**, 5653–5658.

3 J. Velíšek and K. Cejpek, Biosynthesis of food constituents: Vitamins 2. water-soluble vitamins: part 1-A review, *Czech J. Food Sci.*, 2007, **25**, 49–64.

4 J. Liu, Z. Chen, D. Tang, *et al.* Graphene quantum dots-based fluorescent probe for turn-on sensing of ascorbic acid, *Sens. Actuators, B*, 2015, **212**, 214–219.

5 X. Wang, P. Wu, X. Hou, *et al.* An ascorbic acid sensor based on protein-modified Au nanoclusters, *Analyst*, 2013, **138**, 229–233.

6 H. Meng, X. Zhang, C. Yang, *et al.* Efficient two-photon fluorescence nanoprobe for turn-on detection and imaging of ascorbic acid in living cells and tissues, *Anal. Chem.*, 2016, **88**, 6057–6063.

7 J. Lykkesfeldt, Determination of ascorbic acid and dehydroascorbic acid in biological samples by high-performance liquid chromatography using subtraction methods: reliable reduction with tris[2-carboxyethyl] phosphine hydrochloride, *Anal. Biochem.*, 2000, **282**, 89–93.

8 A. G. Frenich, M. E. H. Torres, A. B. Vega, *et al.* Determination of ascorbic acid and carotenoids in food commodities by liquid chromatography with mass spectrometry detection, *J. Agric. Food Chem.*, 2005, **53**, 7371–7376.

9 J. K. Kwakye, The use of stabilizers in the UV assay of ascorbic acid, *Talanta*, 2000, **51**, 197.

10 G. Wang, Z. Chen and L. Chen, Mesoporous silica-coated gold nanorods: towards sensitive colorimetric sensing of ascorbic acid *via* target-induced silver overcoating, *Nanoscale*, 2011, **3**, 1756–1759.

11 L. He, F. Wang, Y. Chen, *et al.* Rapid and sensitive colorimetric detection of ascorbic acid in food based on the intrinsic oxidase-like activity of MnO_2 nanosheets, *Luminescence*, 2018, **33**, 145–152.

12 S. A. Kumar, P. H. Lo and S. Chen, Electrochemical selective determination of ascorbic acid at redox active polymer modified electrode derived from direct blue 71, *Biosens. Bioelectron.*, 2008, **24**, 518–523.

13 X. Cao, L. Luo, Y. Ding, *et al.* Electrochemical methods for simultaneous determination of dopamine and ascorbic acid using cetylpyridine bromide/chitosan composite film-modified glassy carbon electrode, *Sens. Actuators, B*, 2008, **129**, 941–946.

14 S. Huang, F. Zhu, Q. Xiao, *et al.* A CdTe/CdS/ZnS core/shell/shell QDs-based "OFF–ON" fluorescent biosensor for sensitive and specific determination of L-ascorbic acid, *RSC Adv.*, 2014, **4**, 46751–46761.

15 L. Zhang, G. Wang, D. Wu, *et al.* Highly selective and sensitive sensor based on an organic electrochemical transistor for the detection of ascorbic acid, *Biosens. Bioelectron.*, 2018, **100**, 235–241.

16 Y. Dong, T. Gao, X. Chu, *et al.* Flow injection-chemiluminescence determination of ascorbic acid based on luminol–ferricyanide–gold nanoparticles system, *J. Lumin.*, 2014, **154**, 350–355.

17 Y. Ma, M. Zhou, X. Jin, *et al.* Flow-injection chemiluminescence determination of ascorbic acid by use of the cerium(IV)–Rhodamine B system, *Anal. Chim. Acta*, 2002, **464**, 289–293.

18 Z. Zhang, H. Cui, C. Lai, *et al.* Gold nanoparticle-catalyzed luminol chemiluminescence and its analytical applications, *Anal. Chem.*, 2005, **77**, 3324–3329.

19 Z. Wang, X. Teng and C. Lu, Carbonate interlayered hydrotalcites-enhanced peroxynitrous acid

chemiluminescence for high selectivity sensing of ascorbic acid, *Analyst*, 2012, **137**, 1876–1881.

20 D. Ji, Y. Du, H. Meng, *et al.* A novel colorimetric strategy for sensitive and rapid sensing of ascorbic acid using cobalt oxyhydroxide nanoflakes and 3,3′,5,5′-tetramethylbenzidine, *Sens. Actuators, B*, 2018, **256**, 512–519.

21 N. Li, Y. Li, Y. Han, *et al.* A highly selective and instantaneous nanoprobe for detection and imaging of ascorbic acid in living cells and in vivo, *Anal. Chem.*, 2014, **86**, 3924–3930.

22 W. Cui, Y. Wang, D. Yang, *et al.* Fluorometric determination of ascorbic acid by exploiting its deactivating effect on the oxidase–mimetic properties of cobalt oxyhydroxide nanosheets, *Mikrochim. Acta*, 2017, **184**, 4749–4755.

23 J. Liu, D. Tang, Z. Chen, *et al.* Chemical redox modulated fluorescence of nitrogen-doped graphene quantum dots for

probing the activity of alkaline phosphatase, *Biosens. Bioelectron.*, 2017, **94**, 271–277.

24 Q. Cai, J. Li, J. Ge, *et al.* A rapid fluorescence "switch-on" assay for glutathione detection by using carbon dots–MnO$_2$ nanocomposites, *Biosens. Bioelectron.*, 2015, **72**, 31–36.

25 K. K. Lee, P. Y. Loh, C. H. Sow, *et al.* CoOOH nanosheet electrodes: simple fabrication for sensitive electrochemical sensing of hydrogen peroxide and hydrazine, *Biosens. Bioelectron.*, 2013, **39**, 255–260.

26 A. D. Jagadale, D. P. Dubal and C. D. Lokhande, Electrochemical behavior of potentiodynamically deposited cobalt oxyhydroxide (CoOOH) thin films for supercapacitor application, *Mater. Res. Bull.*, 2012, **47**, 672–676.